



Jul 1st, 12:00 AM

Emissions corridors preserving the Atlantic ocean thermohaline circulation

K. Zickfeld

T. Bruckner

Follow this and additional works at: <https://scholarsarchive.byu.edu/iemssconference>

Zickfeld, K. and Bruckner, T., "Emissions corridors preserving the Atlantic ocean thermohaline circulation" (2002). *International Congress on Environmental Modelling and Software*. 193.
<https://scholarsarchive.byu.edu/iemssconference/2002/all/193>

This Event is brought to you for free and open access by the Civil and Environmental Engineering at BYU ScholarsArchive. It has been accepted for inclusion in International Congress on Environmental Modelling and Software by an authorized administrator of BYU ScholarsArchive. For more information, please contact scholarsarchive@byu.edu, ellen_amatangelo@byu.edu.

Emissions corridors preserving the Atlantic ocean thermohaline circulation

K. Zickfeld^a, T. Bruckner^b

^a*Potsdam Institute for Climate Impact Research, D-14473 Potsdam, Germany
(Kirsten.Zickfeld@pik-potsdam.de)*

^b*Institute for Energy Engineering, Technical University of Berlin, D-10587 Berlin, Germany*

Abstract:

The Atlantic thermohaline circulation (THC) transports large amounts of heat northward, acting as a heating system for the northern North Atlantic and north-western Europe. Paleo-reconstructions and a large number of model simulations have shown the THC to be stable only within certain limits beyond which the circulation shuts down. In this paper we derive emission corridors for the 21st century preserving the Atlantic thermohaline circulation. To this end a multi-gas reduced-form climate model has been coupled to a dynamic four-box model of the Atlantic thermohaline circulation. Both models allow for the relevant uncertainties (i.e., climate and hydrological sensitivity) to be taken into account. The emission corridors are calculated along the conceptual and methodological lines of the tolerable windows approach. The corridor boundaries demarcate time-dependent limits beyond which either the THC collapses or the mitigation burden to avoid such an event becomes intolerable. Accordingly, the corridors represent the maneuvering space for any climate policy committed to preserve the THC without endangering future economic growth. Results show a large dependence of the width of the emission corridors on hydrological sensitivity, which is a measure for the amount of additional freshwater entering the North Atlantic, and on climate sensitivity.

Keywords: climate change, tolerable windows approach, emissions corridors, sensitivity analysis

1 INTRODUCTION

Potentially unstable features of the climate system are gaining increasing scientific and public attention, because they could be the origin of major and rapid disruptions of the human life support systems. A prominent example for this is a conceivable breakdown of the Atlantic thermohaline circulation (THC), i.e., that part of the Atlantic ocean circulation which is driven by density gradients. This circulation transports large amounts of heat northward (in the order of $1 \text{ PW} = 10^{15} \text{ W}$), acting as a heating system for north-western Europe and the northern North Atlantic. Paleo-reconstruction [Dansgaard et al., 1993] and model simulations [Manabe and Stouffer, 1993] have shown the potential for a thermohaline circulation instability and raised the concern that global climate change may trigger a transition into a circulation state without deep water

formation in the Atlantic. Because of the possibly severe consequences that a collapse of the THC could bring about, this event may be considered as a ‘dangerous anthropogenic interference with the climate system’ that Article 2 of the United Nations Framework Convention on Climate Change (UNFCCC) calls to avoid. The aim of this paper is to present emissions corridors which keep the THC in its present mode of operation, while considering expectations about the socio-economically acceptable pace of emissions reductions efforts.

2 METHODOLOGY AND MODEL COMPONENTS

Emissions corridors represent the ranges of long term CO₂ greenhouse gas emissions which are allowed under a predefined set of normative climate policy goals (or ‘guard-rails’). They are calculated

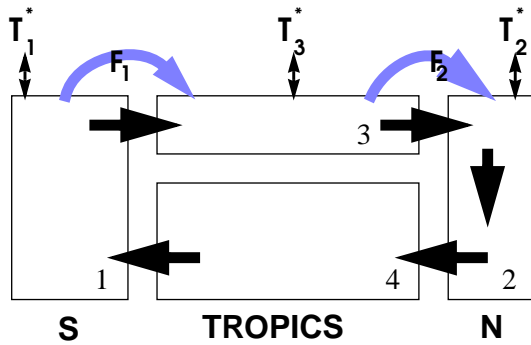


Figure 1: Schematic of the four-box model of the Atlantic thermohaline circulation. The temperatures of boxes 1,2,3 are relaxed toward the values T_1^* , T_2^* , and T_3^* , respectively. The salinities are forced by the freshwater fluxes F_1 and F_2 . The meridional flow (black arrows) is proportional to the density gradient between boxes 1 and 2.

along the conceptual and methodological lines of the tolerable windows approach (TWA, or ‘guard-rail’ approach, [Bruckner et al., 1999]). The analytical tool used for the scope of this paper consists of a box model of the THC coupled to a reduced-form climate model. We rely on simple representations of the climate system because of the high computational costs of the procedure used for the computation of the emissions corridors. The latter is implemented as a specially formulated dynamic control problem. The time evolution of the coupled anthroposphere-ocean-atmosphere system is described by a set of differential equations $\dot{\mathbf{x}}(t) = \mathbf{f}(\mathbf{x}(t), \mathbf{u}(t), t)$, subject to the initial conditions $\mathbf{x}(t=0) = \mathbf{x}_0$. $\mathbf{x}(t)$ is the state vector of the system, and $\mathbf{u}(t)$ is the control vector. In our specific analysis the state vector $\mathbf{x}(t)$ includes variables like global mean temperature, concentrations of all major greenhouse gases, and the Atlantic circulation strength. The control vector $\mathbf{u}(t)$ comprises the level of industrial CO_2 emissions. The guard-rails impose exogenous environmental, climatic, and economic constraints on the evolution of the system. They are described by constraint functions of the form $h(\mathbf{x}(t), \mathbf{u}(t), t) \leq 0$, which imply restrictions on the state and control variables. Here, the goal of preserving the THC is implemented by constraining the Atlantic overturning to remain above the critical flow m_{crit} (i.e., the flow strength beyond which the THC would inevitably collapse, which approximately equals half of the initial overturning [Rahmstorf, 1996]). Further, we express expectations about the socio-economically acceptable pace of emissions reductions efforts by imposing a constraint on the maximum admissible rate of emis-

sions reductions r , and by requiring a time span t_{trans} for the transition towards a de-carbonizing economy (for a detailed discussion of the economically motivated guard-rails see [Kriegler and Bruckner, 2002]). The goal of our analysis is to identify the complete bundle of control paths $\mathbf{u}(\cdot)$ and corresponding state trajectories $\mathbf{x}(\cdot)$ which are consistent with the set of differential equations $\dot{\mathbf{x}}(t) = \mathbf{f}(\mathbf{x}(t), \mathbf{u}(t), t)$, subject to $\mathbf{x}(t=0) = \mathbf{x}_0$ and the constraints $h(\mathbf{x}(t), \mathbf{u}(t), t) \leq 0$. A suitable mathematical framework for the determination of the set-valued solution to this problem is the theory of differential inclusions [Aubin, 1991]. Although determining the full solution (i.e., the totality of admissible bundles) is not feasible at the current state of this theory, it is possible to derive interesting properties of these bundles. For example, a combination of concepts from the field of differential inclusions and control theory allows for the determination of the outer boundaries of the admissible control space [Leimbach and Bruckner, 2001]. The area between these boundaries is what is referred to as ‘emissions corridor’. Concretely, the upper (lower) boundary of the emissions corridor is derived by subsequently maximizing (minimizing) CO_2 emissions for fixed time t . Fig. 3 illustrates this algorithm by displaying paths maximizing emissions in the years 2020, 2060, 21000. The entire upper (lower) boundary is put up by the maxima (minima) of such emissions paths.

2.1 Atlantic thermohaline circulation model

The THC model is a cross-hemispheric extension of the seminal Stommel box model [Stommel, 1961]. It consists of four well-mixed boxes, which represent the southern, tropical, northern and deep Atlantic (Fig. 1) [Rahmstorf, 1996]. The surface boxes are coupled to the overlying atmosphere through fluxes of heat and freshwater. Assuming modern ocean conditions, i.e., the water in the northern box being denser than that in the southern box, a pressure-driven circulation develops with northward flow at the surface and southward flow at depth. The dynamics of the system is described by a set of differential equations for temperatures and salinities of each of the four boxes, which adjust to the transport of heat and salt by the circulation and to the atmospheric fluxes of heat and freshwater. The meridional flow is proportional to the density gradient between the northern and the southern box. The box model was fitted to modern ocean conditions by comparison with results obtained with the coupled CLIMBER-2 model [Petoukhov et al., 2000]. We use the model to diagnose the response of the At-

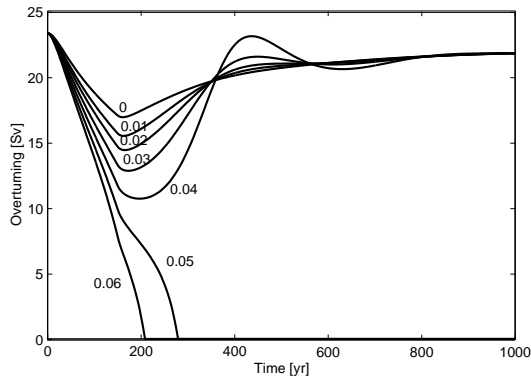


Figure 2: Response of the Atlantic overturning to a linear increase in global mean temperature ($4.5\text{ }^\circ\text{C}$ over 150 years, then constant) for different values of the North Atlantic hydrological sensitivity [$\text{Sv}/^\circ\text{C}$] ($1\text{Sv}=10^6\text{ m}^3\text{s}^{-1}$).

Atlantic overturning (i.e., the volume transport, a measure for the strength of the circulation) to scenarios of global mean temperature change (ΔT^{GL}), which is the output of the climate model described in section 2.2. These scenarios have to be appropriately down-scaled into basin-wide patterns of changes in sea surface temperature (ΔT_i^*) and net freshwater fluxes (ΔF_i) to drive the THC model. This is achieved by assuming a linear relationship between changes in the spatial patterns and global mean temperature change:

$$\Delta T_i^* = p_i \Delta T^{GL}, \quad i \in \{1, 2, 3\} \quad (1)$$

$$\Delta F_1 = h_1 \Delta T^{SH} = h_1 p^{SH} \Delta T^{GL}, \quad (2)$$

$$\Delta F_2 = h_2 \Delta T^{NH} = h_2 p^{NH} \Delta T^{GL}, \quad (3)$$

where T^{SH} and T^{NH} are the mean temperatures of the southern and northern Hemisphere, respectively, and h_i , p_i are proportionality constants, whose standard values are listed in Table 1. The h_i are in the following referred to as ‘hydrological sensitivities’ (in particular, h_2 as ‘North Atlantic hydrological sensitivity’). Although simple, the model is able to reproduce key dynamic features of complex climate models (see Fig. 2). In response to low temperature change scenarios, for example, the circulation is weakened and, as soon as temperatures are stabilized, recovers. This is in line with recent the behaviour of a complex coupled climate model found by Stouffer and Manabe [1999]. For high temperature change scenarios, or scenarios with a high value of the North Atlantic hydrological sensitivity, the circulation shuts down, indicating the existence of a threshold value in the freshwater forcing beyond

Climate change scenario parameters	
Regional temperature constants:	
p_1	0.91
p_2	1.07
p_3	0.79
p^{SH}	0.95
p^{NH}	1.08
Hydrological sensitivities:	
h_1	$0\text{ Sv}^\circ\text{C}^{-1}$
h_2	$0.03\text{ Sv}^\circ\text{C}^{-1}$
Climate sensitivity:	
$T_{2 \times CO_2}$	$2.5\text{ }^\circ\text{C}$

Table 1: Standard model parameters (see Eq. 1-3).

which circulation cannot be sustained. The latter is similar to the behaviour seen in experiments by, e.g., Rahmstorf and Ganopolski [1999] and Manabe and Stouffer [1993]. Further, we found response of the overturning in our box model to be sensitive to the rate of temperature increase as described by Stocker and Schmittner [1997] (not shown).

2.2 Climate model

For the computation of global mean temperature we use a multi-gas reduced-form model capable of mimicking the behavior of sophisticated three dimensional general circulation models [Bruckner et al., 2002]. The model translates anthropogenic emissions of CO_2 , CH_4 , N_2O , halocarbons, SF_6 and SO_2 into the corresponding atmospheric concentrations and further into radiative forcing and near-surface global mean temperature. Its core component is a differential analogue to a non-linear impulse response function model of the coupled carbon-cycle-plus-climate system which explicitly takes into account ocean carbon chemistry and the terrestrial biosphere. For the modeling of the atmospheric chemistry and radiative forcing of non- CO_2 greenhouse gases and aerosols various components of the MAGICC model have been adopted [Wigley, 1994]. The model can be applied with different values for the climate sensitivity.

3 RESULTS

In the following we present emissions corridors compatible with the goal of preserving the THC. We first calculated the emissions corridor for standard model settings and then performed sensitivity analyses with respect to the main uncertain param-

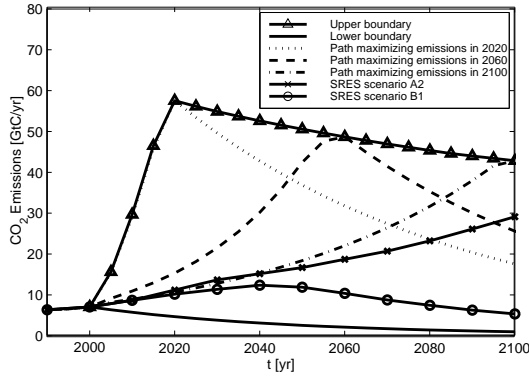


Figure 3: Emissions corridors (area between upper and lower boundary) for standard parameter settings (see Table 1). For illustration of its internal structure we show paths maximizing CO₂ emissions in 2020, 2060, and 2100. For reference we also display a high and a low emissions scenario (SRES marker scenarios A2 and B1, respectively).

eters, such as climate sensitivity and North Atlantic hydrological sensitivity. The ‘standard’ parameter values are shown in Table 1. Further, CO₂ emissions from land-use change and emissions of non-CO₂ greenhouse gases are assumed to follow the average of the four SRES marker scenarios (i.e., the average of A1, A2, B1, B2, [Nakićenović and Swart, 2000]) until 2100, and are then held constant. SO₂ emissions are linked to industrial CO₂ emissions (i.e., the control variable) assuming a globally averaged desulfurization rate of 1.5% per year. As far as the THC guard-rail and the socio-economic motivated constraints are concerned (see section 2), we set the minimum admissible flow rate m_{crit} to 10 Sv, the maximum rate of global emissions reductions r to 2% per year and the transition time t_{trans} to 20 years. The resulting corridor is displayed in Fig. 3, along with selected emissions paths to illustrate its internal structure. It follows from the conceptual foundation of the TWA that any given point lying within the corridor can be reached by at least one admissible emission path, but an arbitrary path inside the corridor is not necessarily admissible. For example, the upper boundary of the corridor can be reached in 2060 only if emissions remain far inside the corridor for several decades in the first half of the 21st century. For reference Fig. 3 also displays a low and a high CO₂ emission scenario (SRES scenario B1 and A2, [Nakićenović and Swart, 2000]). We find that for standard parameter values the emissions corridor is wider than the range spanned by the SRES emissions scenarios. In the following, however, we show that this

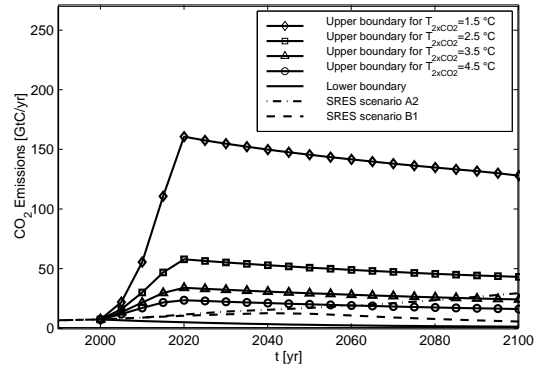


Figure 4: Emissions corridor for different values of climate sensitivity $T_{2 \times CO_2}$. The lower corridor boundary is the same for all values of $T_{2 \times CO_2}$, as it is solely determined by the maximum emissions reduction rate r .

result is very sensitive to the specific assumptions made about climate and hydrological sensitivities. In terms of CO₂ concentrations and global mean temperature the imposed guard-rails imply a maximum of approximately 1300 ppm reached during the 22nd century followed by a slight decline thereafter and a stabilization at around 5.5 °C, respectively (not shown).

Fig. 4 displays emissions corridors for different values of climate sensitivity $T_{2 \times CO_2}$. The latter parameter is varied in the range 1.5 to 4.5 °C (with all other parameters at their standard values), which is the uncertainty range given by the IPCC in its Second Assessment Report [Kattenberg et al., 1995]. Our findings indicate a very strong dependence of the width of the emissions corridor on climate sensitivity. This sensitivity affects only the position of the upper corridor boundary, as the lower one is solely determined by the maximum emissions reduction rate r and thus is the same for all values of climate sensitivity. For a value of 1.5 °C the upper corridor boundary is far from being touched by the emissions projected for the 21st century by the SRES emissions scenarios. For a climate sensitivity of 2.5 °C the upper boundary is still out of reach, but the width of the corridor is considerably reduced (by approximately 60%). For climate sensitivities of 3.5 and 4.5 °C the corridors shrink further, and the high reference emissions scenario (SRES marker scenario A2) crosses the upper corridor boundaries. It must be emphasized that a transgression of the corridor boundaries does not imply an immediate collapse of the THC: because of the inertia of the ocean, the actual event occurs centuries after it is

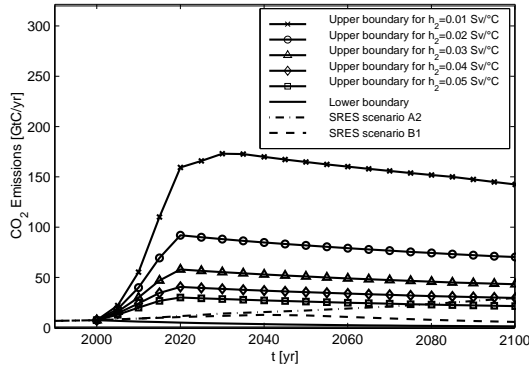


Figure 5: Emissions corridor for different values of the North Atlantic hydrological sensitivity h_2 (with all other parameters at their standard values).

triggered. Two mechanisms contribute in our model to the reduction of the corridor with increasing climate sensitivity: the differential warming between the southern and the northern boxes (compare the values for p_1 and p_2 in Table 1), and the enhanced freshwater transport towards the northern latitudes, which increases with growing global mean temperature (see Eq. 3). Both act to reduce the meridional density gradient which drives the THC and thus make the latter more sensitive.

Further, we computed emissions corridors for different values of the North Atlantic hydrological sensitivity h_2 , which is among the main uncertainties in predicting the fate of the THC. The reason is that estimates of evaporation and precipitation changes over the North Atlantic differ largely between models, as well as estimates of freshwater runoff from the Greenland ice sheet and other melting glaciers in the North Atlantic catchment. Here we assume an uncertainty range for h_2 of 0.01-0.05 Sv/°C (for a justification see [Rahmstorf and Ganopolski, 1999]). Fig. 5 shows emissions corridors for different values of the North Atlantic hydrological sensitivity. As for climate sensitivity, the size of the emissions corridors largely depends on the specific parameter choice: for low values of h_2 the corridor is much larger than the range spanned by the SRES emissions scenarios, while for high values SRES emissions scenario A2 transgresses the upper corridor boundary. This strong sensitivity of the THC to the value of the North Atlantic hydrological sensitivity h_2 was already indicated in Fig. 2: the higher h_2 , the more additional freshwater enters the North Atlantic for a given amount of warming and thus the closer the circulation gets to the critical threshold. Assuming the values 1.5 to

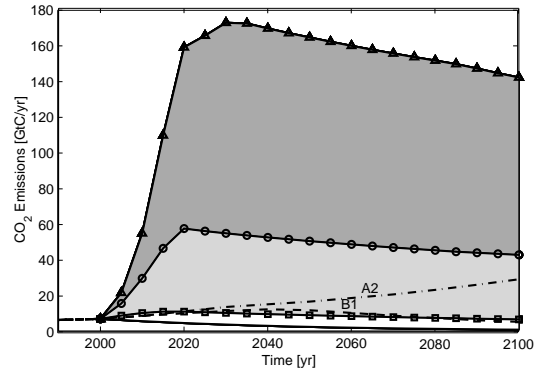


Figure 6: Emissions corridor for the 'best case' (triangles), 'best guess' (circles), and 'worst case' (squares) combination of model parameter values. The shaded areas between the corridors indicate likelihood domains for a shutdown of the THC: the darker the shading, the higher the probability that any given emissions paths entering that domain triggers a breakdown of the THC. For reference we show a high and a low emissions scenario (SRES marker scenarios A2 and B1, respectively).

4.5 °C for climate sensitivity and the values 0.01-0.05 Sv/°C for hydrological sensitivity as spanning the complete ranges of parameter values, we calculated emissions corridors for the 'best case', 'best guess', and 'worst case' combination of model parameters. As 'best-guess' we refer to the combination $T_{2 \times CO_2} = 2.5$ °C, $h_2 = 0.03$ Sv/°C, which corresponds to the standard settings of our model. The results are displayed in Fig. 6. For the 'best case' the upper corridor boundary is far from being touched by any emissions scenario for the 21st century. As discussed previously, for the 'best guess' case the corridor is larger than the range spanned by the SRES emissions scenarios. For the 'worst case' combination of model parameters, the corridor almost vanishes. This implies that, given the amount of greenhouse gases already in the atmosphere, and the inertia of the climate system, the maneuvering space for any climate policy committed to the precautionary principle is extremely tight. Indeed, even the non-intervention low emissions scenario B1 leaves the area of the 'worst case' corridor, emphasizing the necessity to abandon the range of conceivable business-as-usual paths as soon as possible. The leeway could be enlarged if mitigation options for non-CO₂ greenhouse gases were considered or the expectations about the socio-economically acceptable pace of CO₂ emissions reduction were relaxed (i.e., t_{trans} decreased and r increased). The shaded areas in Fig. 6 may be interpreted as likeli-

hood domains for a collapse of the THC: the darker the shading of the area that any given emissions scenario enters, the higher the probability that a complete and irreversible breakdown of the THC is triggered.

4 CONCLUSIONS

The analysis presented in this paper aimed at identifying the leeway for action for any policy committed to the preservation of the Atlantic thermohaline circulation without endangering future economic growth. We found that for the ‘best guess’ choice of model parameters, the CO₂ emissions corridor is larger than the range spanned by the SRES emissions scenarios for the 21st century. We then tested the robustness of these findings by performing a sensitivity analysis with respect to the main uncertain quantities in projecting the fate of the THC, i.e., climate and North Atlantic hydrological sensitivity. We found that the width of the emissions corridor is largely dependent upon the specific parameter choices: for small values of climate and hydrological sensitivities the upper corridor boundary is far from being reached by any of the SRES emissions scenarios, while for high values of both parameters the corridor area is considerably tightened, such that even low non-intervention emissions scenarios would transgress the upper corridor boundary.

5 REFERENCES

Aubin, J. *Viability theory*. Birkhaeuser, Basel, 1991.

Bruckner, T., G. Hooss, H. Fuessel, and K. Hasselmann. Climate system modeling within the framework of the tolerable windows approach: the ICLIPS climate model. *Climatic Change*, forthcoming, 2002.

Bruckner, T., G. Petschel-Held, F. Tóth, H. Fuessel, C. Helm, M. Leimbach, and H. Schellnhuber. Climate change decision support and the tolerable windows approach. *Environmental Modeling and Assessment*, 4:217–234, 1999.

Dansgaard, W., S. Johnsen, H. Clausen, N. Dahl-Jensen, N. Gundestrup, C. Hammer, C. Hvidberg, J. Steffensen, A. Sveinbjornsdottir, J. Jouzel, and G. Bond. Evidence for general instability of past climate from a 250-kyr ice-core record. *Nature*, 364:218–220, 1993.

Kattenberg, A., F. Giorgi, H. Grassl, G. Meehl, J. Mitchell, R. Stouffer, T. Tokioka, A. Weaver, and T. Wigley. Climate models - Projections of

future climate. In Houghton, J., L. M. Filho, B. Callander, N. Harris, A. Kattenberg, and K. Maskell, editors, *Climate Change 1995: The science of climate change - Contribution of Working Group I to the Second Assessment Report of the IPCC*, pages 285–357. Cambridge University Press, Cambridge, 1995.

Kriegler, E. and T. Bruckner. Sensitivity analysis of emissions corridors for the 21st century. *Climatic Change*, submitted, 2002.

Leimbach, M. and T. Bruckner. Influence of economic constraints on the shape of emission corridors. *Computational Economics*, 18:173–191, 2001.

Manabe, S. and R. J. Stouffer. Century-scale effects of increased atmospheric CO₂ on the ocean-atmosphere system. *Nature*, 364:215–218, 1993.

Nakićenović, N. and R. Swart. *Emissions scenarios*. Cambridge University Press, Cambridge, 2000.

Petoukhov, V., A. Ganopolski, V. Brovkin, M. Claussen, A. Eliseev, C. Kubatzki, and S. Rahmstorf. CLIMBER-2: a climate system model of intermediate complexity. Part I: model description and performance for present climate. *Climate Dynamics*, 16:1–17, 2000.

Rahmstorf, S. On the freshwater forcing and transport of the Atlantic thermohaline circulation. *Climate Dynamics*, 12:799–811, 1996.

Rahmstorf, S. and A. Ganopolski. Long-term global warming scenarios computed with an efficient coupled climate model. *Climatic Change*, 43: 353–367, 1999.

Stocker, T. F. and A. Schmittner. Influence of CO₂ emission rates on the stability of the thermohaline circulation. *Nature*, 388:862–865, 1997.

Stommel, H. Thermohaline convection with two stable regimes of flow. *Tellus*, 13:224–241, 1961.

Stouffer, R. J. and S. Manabe. Response of a coupled ocean-atmosphere model to increasing atmospheric carbon dioxide: sensitivity to the rate of increase. *Journal of Climate*, 12:2224–2237, 1999.

Wigley, T. *MAGICC (Model for the assessment of greenhouse-gas induced climate change): User’s guide and scientific reference manual*. National Center for Atmospheric Research, Boulder, Colorado, 1994.